Bi-directional locomotion of a magnetically-actuated jellyfish-inspired soft robot

Pramanik, Ratnadeep; Onck, Patrick R.; Verstappen, Roel W.C.P.

Published in:
Advances in Robotics, AIR 2021 - 5th International Conference of the Robotics Society

DOI:
10.1145/3478586.3478591

Bi-directional locomotion of a magnetically-actuated jellyfish-inspired soft robot

Ratnadeep Pramanik
Computational Mechanics and Numerical Mathematics Group, University of Groningen, Groningen, NetherlandsMicromechanics Group, University of Groningen, Groningen, Netherlands

Patrick Raymond Onck
Micromechanics Group, University of Groningen, Groningen, Netherlands

Roel W. C. P. Verstappen
Computational Mechanics and Numerical Mathematics Group, University of Groningen, Groningen, Netherlands

ABSTRACT

Biomimetic compliant untethered robots find a plethora of applications in biomedical engineering, microfluidics, soft robotics, and deep-sea exploration. Flexible miniature robots in the form of magnetically actuated compliant swimmers are increasingly used for targeted drug delivery, robotic surgery, laparoscopy, and microfluidic device design. These applications require an in-depth understanding of the nonlinear large deformation structural mechanics, non-invasive remote-control and untethered actuation mechanisms, and associated fluid-structure interactions that arise between a soft smart robot and its surrounding fluid. The present work obtains numerical solutions for the temporal evolution of structural and flow variables using a fictitious domain method that employs a robust multi-physics computational model involving both fluid-structure interaction and magneto-elasto-dynamics. The magnetically-actuated soft robotic swimmer (jellyfishbot) is inspired by the most efficient aquatic swimmer, the jellyfish. The swimming kinematics and bi-directional locomotion are obtained for different waveforms and gradients of the external magnetic actuation. The breaking of temporal symmetry and its relative dominance is discussed as well.

CCS CONCEPTS

• **Applied Computing**; • **Physical Sciences and Engineering**; • **Physics**;

KEYWORDS

Jellyfish-inspired, soft robot, swimming kinematics, magnetically-actuated, bi-directional locomotion

ACM Reference Format:

Ratnadeep Pramanik, Patrick Raymond Onck, and Roel W. C. P. Verstappen. 2021. Bi-directional locomotion of a magnetically-actuated jellyfish-inspired soft robot. In *Advances in Robotics - 5th International Conference of The Robotics Society (AIR2021), June 30–July 04, 2021, Kanpur, India.* ACM, New York, NY, USA, 5 pages. https://doi.org/10.1145/3478586.3478591

AIR2021, June 30–July 04, 2021, Kanpur, India

ACM ISBN 978-1-4503-8971-6/21/06.
https://doi.org/10.1145/3478586.3478591

1 INTRODUCTION

Soft robotics has been an actively-growing area of intense and popular research owing to its ever-expanding range of biomedical and health care applications, and use in microfluidic devices [1], [12]. Targeted drug delivery, robotic surgery and laparoscopy are some of the key challenges addressed by soft robots [2]. Flexible robots are ergonomic and possess large degrees of freedom. Generally, these are made of shape memory polymers [7], soft pneumatic composites [8], or soft magnetic elastomeric composites [9]. Magnetically-actuated soft robots are often desired to locomote through viscous fluids in the form of untethered swimmers for different biomedical applications, during which they undergo strong fluid-structure interaction [6], [13]. Such a jellyfish-inspired soft swimmer robot [3] is studied for its biomimetic computational design and swimming kinematics. The proposed model studies the jellyfishbot kinematics and swimming bi-directionality using numerical experiments. Although dynamic models [9] or CFD-based approaches [14] have been undertaken, there exists a lacuna in the development of a robust, coupled large deformation fluid-structure interaction multi-physics computational framework that includes the full Navier-Stokes and magneto-elasto-dynamics. Also, bi-directionality has been reported in only a few specific cases such as magnetically-actuated flagella [16]. The present works seeks to address these shortcomings in a holistic manner.

2 PROBLEM FORMULATION

The jellyfishbot (Fig. 1a) swims through a viscous fluid and is capable of shape-morphing under external magnetic fields (B_o). Magnetic actuation ensures a non-invasive approach with high precision, control and manoeuvring [3]. Magnetic filler materials are added into a polymer matrix to obtain a flexible smart composite [9]. Permanently magnetic microparticles (NdFeB, avg. dia. 5 μm) embedded in an elastomer (Silicone) in equal mass ratios (1:1) with an isotropic material distribution yields a soft magnetic composite with magneto-responsive features [3].

The structural, fluid and magnetic properties considered for numerical simulation are reported in Table. 1. These values are motivated from a recent work reported on artificial magnetically-actuated jellyfishbot [3], [9]. A dynamic model has been proposed in [9] to study the jellyfishbot swimming kinematics and performance. However, the present work develops a robust computational multi-physics design methodology for the same objective. Although bi-directionality has not been experimentally demonstrated in [3], ephyra and jellyfishbot architecture, their individual swimming

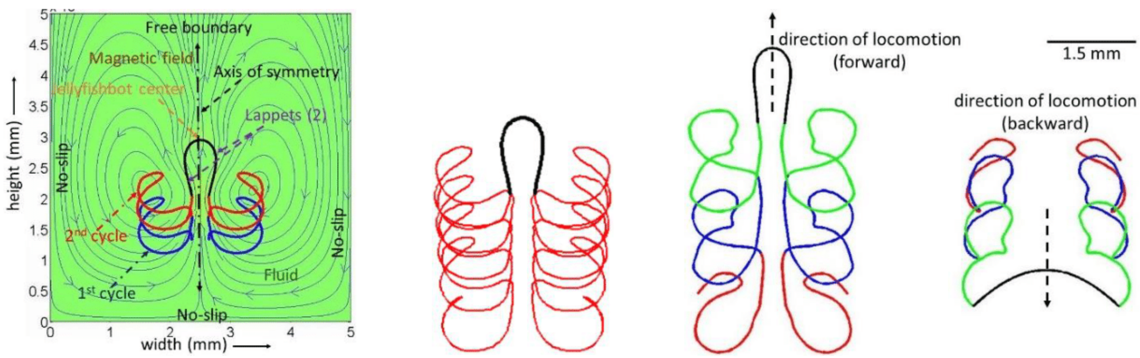

Figure 1: Schematic of the jellyfishbot (a); steady-state kinematics (b); trajectory of three consecutive swimming cycles for jellyfishbot forward (c) and backward (d) locomotion (color – black: jellyfishbot, red: first cycle, blue: second cycle and green: third cycle)

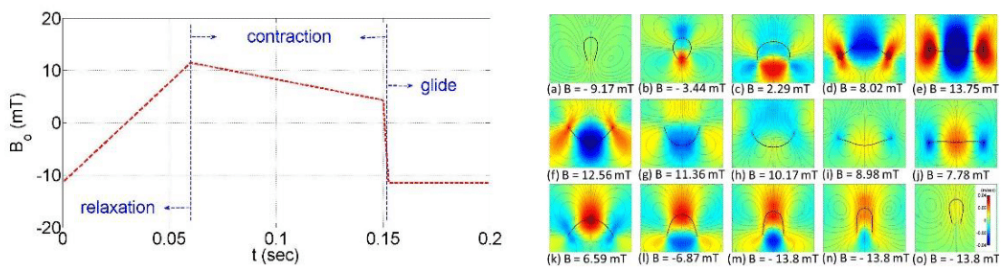

Figure 2: Variation of B_o with time (left); motion kinematics: relaxation (a) – (f), contraction (g) – (l) and glide (m) – (o) phases (right)

Table 1: Jellyfishbot material and geometric properties, magnetic parameters and surrounding fluid properties (motivated from [3])

Parameter	Symbol	Value	Unit
Young's Modulus	E	0.2	MPa
Density	ρ_s	1500	kg/m^3
Length	L	3.0	Mm
Thickness	h	0.065	Mm
Fluid density	ρ_f	1500	kg/m^3
Viscosity	μ	0.01	Pa. sec
Remnant Magnetization	$M_{r,t}$	30.37 + f(ϕ)	kA/m
	$M_{r,n}$	-3.86 + g(ψ)	kA/m

kinematics, lappet strokes and different modes of locomotion have been vividly discussed. Steady-state motion kinematics for the jellyfishbot is schematically shown in Fig. 1 (b). This is to demonstrate a similar lappet trajectory for each swimming cycle and ensure repeatability. A soft-bodied ephyra has eight soft lappets that deform symmetrically. The computationally-designed jellyfishbot is considered to be two-dimensional and it has two lappets that deform symmetrically (Fig. 2). Both the ephyra and the jellyfishbot have three phases during one swimming cycle: relaxation, contraction and glide [4], [5]. During relaxation, the jellyfish widens and opens up its lappets. The reverse takes place during contraction. During the glide phase, there is no observable lappet deformation.

3 JELLYFISH(BOT) MOTION KINEMATICS

The external oscillating magnetic field always acts along the longitudinal direction. During the relaxation phase, B_o gradient (i.e., the slope of the magnetic field B_o) is positive (Fig. 2). The magnetic body couple thus generated deforms the lappets upwards in a symmetric manner about the jellyfishbot center. The lappets push the surrounding fluid upwards, thereby causing the jellyfishbot to traverse downwards (Figs. 1 and 2). During the contraction phase, B_o gradient is negative. The lappets re-open and deform downwards, which pushes the surrounding fluid downward to generate the thrust required for forward locomotion. B_o gradient is zero during the glide phase: body couple is not generated. The glide phase uses the inertia gained previously in order to traverse some further distance (Fig. 2). When the effective and recovery strokes have dissimilar lappet trajectories, it gives rise to trajectory asymmetry [10]. This is predominantly observed for low values of Reynolds number (R_e < 1). When the effective stroke is quicker compared to the recovery stroke, the lappets displace more fluid during the former compared to the latter, giving rise to the temporal symmetry and glide [10]. This is observed for moderate to high R_e flow (> 1). In the present study, the R_e is 6.75, which indicates that the temporal asymmetry is dominant.

The sheer dominance of a swimming phase is a consequence of both the B_o gradient, and the time duration of that phase. Higher the B_o gradient and/or quicker the stroke, the more dominant it is. This is owing to the breaking of temporal symmetry and add-on inertial effects [10]. When the relaxation phase dominates, the temporal asymmetry causes the jellyfishbot to locomote in the reverse direction, and vice-versa (Figs. 1c and 1d). The directionality also depends on the relative location of the glide phase. When the glide phase is at the end (Fig. 3), the jellyfishbot locomotes forward. When it is intermediate (Fig. 4), the jellyfishbot traverse backwards. This could again be attributed to the inertial effects that the jellyfishbot utilizes during the glide phase under Stokes drag.

4 COMPUTATIONAL FRAMEWORK

The computational model involving the strongly coupled fluid-lappet interaction with magneto-elasto-dynamics is motivated from [10]. For the ease of numerical modeling, a two-dimensional computational domain is considered (width = height = 5 mm). The jellyfishbot is assumed to be two-dimensional. The out-of-plane dimensions are not considered for the present analysis. The Navier-Stokes's as well as the structural Navier equation have a two-dimensional form. Nevertheless, the kinematic observations can be extrapolated onto a 3D domain, since the deformation pattern and motion kinematics are expected to have the same physics. This aspect shall be dealt in the future endeavor. The top boundary is considered to be a free boundary, whereas the left, right and bottom walls are assumed to be no-slip boundaries. Initial lappet deformation and velocity is zero. The evolution of flow dynamics is governed by the incompressible Navier-Stokes's equation (Eqn. 1). The jellyfishbot lappets are considered as assemblage of Euler-Bernoulli beams with geometric nonlinearity. An updated Lagrangian scheme is adopted, wherein the mesh and structural deformation are updated at every time step. The internal and external virtual works are equated and linearized to obtain the final governing equation (Eqn. 2a) for the structural model [10].

$$\nabla \cdot c = 0, \qquad \rho_f \left[\dot{c} + (\nabla \cdot c)\, c\right] = -\nabla P + 2\mu \nabla \cdot D \tag{1}$$

$$\delta p^T \left(K\Delta p + M\ddot{p}^{t+\Delta t} - F_{ext}^{t+\Delta t} + F_{int}^{t+\Delta t} \right) = 0, \qquad c = \dot{p} \tag{2}$$

$$\nabla \cdot B = 0, \qquad \nabla x\, B = 0, \qquad B = \mu_o (M + H), \qquad N_z = M\, X\, B_o \tag{3}$$

$$\mathrm{f}(\phi) = -32.12 \cos(kx) + 2.231 \sin(kx); \quad \mathrm{g}(\psi) = -53.75 \cos(kx) - 26.25 \sin(kx) \tag{4}$$

No-slip boundary condition (Eqn. 2b) is ensured at the solid-fluid interface through a point-collocation technique using Lagrange multipliers (fictitious domain method) [11], [15]. The numerical solution of the structural kinematics and flow variables are obtained at every time step using an in-house finite element FORTRAN code, TFEM. Maxwell's equations and the appropriate constitutive relation (Eqn. 3) are used to calculate the magnetic body couple N_z at every time step. The remnant magnetization (M_r) has both tangential ($M_{r,t}$) and normal ($M_{r,n}$) components, and the corresponding trigonometric functional dependencies are obtained from [3], [9]. In Eqn. 4), k denotes the phase value of M_r, while x denotes the normalized distance of a point/node from the jellyfishbot center.

5 RESULTS AND DISCUSSION

The default value of actuation frequency (f_m) is 5 Hz. It is observed from the numerical simulations that for the specified values of the structural, fluid and magnetic properties, the jellyfishbot swimming performance degrades upon changing f_m too much. With increase in f_m, the actuation cycle time decreases. This provides lesser time for the robotic swimmer to utilize the glide phase completely, because the next cycle starts sooner than the usual. And when f_m is low, the next cycle starts late. The cyclic actuation is delayed, which again reduces the jellyfishbot swimming performance. The influence of f_m shall be discussed in more detail in the future endeavor, wherein a parametric optimization shall be carried out.

Bi-directional locomotion is schematically shown in Figs. 1c and 1d for three consecutive swimming cycles. A speed of 7.7 and 4.3 mm/sec is observed during forward and backward locomotion, respectively (from Figs. 3 and 4). Indeed, these values can be further augmented with a more-optimized design methodology. However, the present work emphasizes upon the aspect of bi-directional locomotion, which has never been reported till yet for a jellyfishbot, according to the best of author's knowledge!

5.1 Forward locomotion

B_o gradient is manipulated during magnetic actuation to obtain bi-directional swimming. The contraction phase dominates either by quickening the lappet deformation, or increasing the B_o gradient magnitude. The magnetic waveforms that result in forward locomotion are shown in Fig. 3. Two different types of waveforms are considered. In one case (Fig. 3a), all the three phases are present. B_o gradient during contraction phase is gradually altered. With an increase in B_o gradient, the lappets deform faster owing to high magneto-responsiveness. Thus, they do not get sufficient time to utilize the contraction phase in order to push the surrounding fluid to a greater extent. Thus, the average speed reduces, although it locomotes in the forward direction. When B_o gradient decreases, it has more time to push the surrounding fluid downwards and utilize the thrust-based forward propulsion for traversing forward with higher speeds. When B_o gradient during the contraction is high, the lappets do not get considerable time for sweeping higher fluid areas as they are not wide-open to displace higher quantities of fluid (Fig. 3a). For the other actuation type (Fig. 3b), the glide phase is not considered. With a decrease in B_o gradient during relaxation

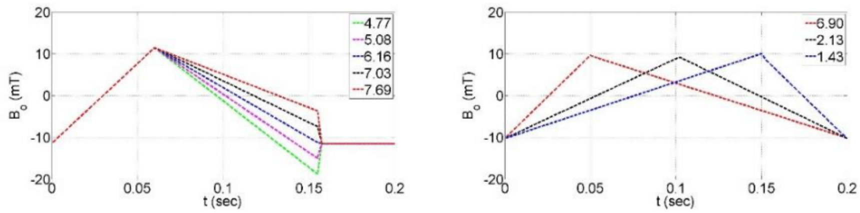

Figure 3: Variation of the jellyfishbot average speed (shown in legend) with change in gradient during the contraction phase(a); and, with no glide phase, and different gradients of the relaxation and contraction phases (b)

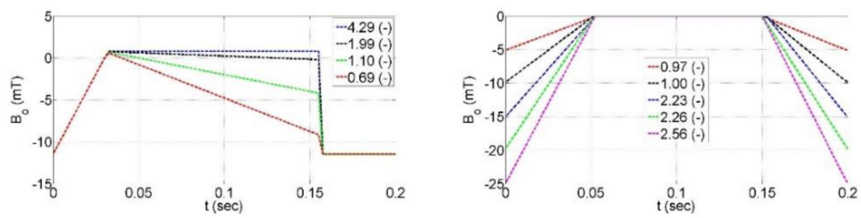

Figure 4: Variation of the jellyfishbot average speed (shown in legend) with different actuation gradients during the contraction phase (a); and, with varying gradients during the relaxation and contraction phases, for a ramp-and-hold magnetic actuation (b)

phase, or its increase during contraction phase, the jellyfishbot speed reduces due to lower inertial effects (Fig. 3b).

5.2 Backward locomotion

The magnitude of B_o gradient is lowered to an upper maximum of zero. With this decrease particularly during the contraction phase, the relative influence of the relaxation phase increases, in the form of maintaining the inertia gained during the previous phase. This results in an enhanced backward swimming kinematics. This is in conjunction with Fig. 4a, where a backward swimming kinematics observed to be the highest when the B_o gradient of the magnetic actuation is zero (during the contraction phase). In essence, the contraction phase now acts like a shifted glide phase that helps in maintaining the jellyfishbot inertia gained previously. For the other type of magnetic actuation (Fig. 4b), the glide phase is located after the relaxation phase. This helps to add-on the inertia gained during the relaxation phase. The higher the magnitude of the lower limit of the external actuation, the higher is the B_o gradient. This results in an increased amount of fluid displaced upwards during the relaxation phase, and consequently, an improved swimming performance in the backward direction! In this way, the magnetically-actuated jellyfishbot exhibits the versatility of bi-directional locomotion under different external magnetic actuation waveforms. It is hoped that this work shall help design engineers, medical experts and clinicians for targeted drug delivery and other non-invasive biomedical applications involving untethered soft robotic swimmers.

6 CONCLUSION

Swimming kinematics and bi-directional locomotion of a jellyfish-inspired flexible swimmer robot is studied using a robust computational multi-physics framework. Large deformation fluid-structure interaction and magneto-elasto-dynamics with appropriate interface, boundary and initial conditions are discussed. The influences of the magnetic field gradient and waveform are analyzed. The dominance of an individual phase dictates directionality. Temporal asymmetry plays a significant role. When the contraction phase dominates, the jellyfishbot traverses forward. The jellyfishbot locomotes backwards when the relaxation phase is dominant. The relative location of the glide phase affects directionality through add-on inertial effects. Future works shall incorporate the fabrication techniques, experimental validation and three-dimensional extrapolation along with other modes of locomotion.

REFERENCES

[1] Matteo Cianchetti, Cecilia Laschi, Arianna Menciassi, and Paolo Dario. 2018. Biomedical applications of soft robotics. Nature Reviews Materials, 3, 6, 143-153. https://doi.org/10.1038/s41578-018-0022-y

[2] Hakan Ceylan, I Ceren Yasa, Oncay Yasa, A Fatih Tabak, Joshua Giltinan, and Metin Sitti. 2018. 3D-printed biodegradable microswimmer for drug delivery and targeted cell labeling. BioRxiv, 379024. https://doi.org/10.1101/379024

[3] Ziyu Ren, Wenqi Hu, Xiaoguang Dong, and Metin Sitti. 2019. Multi-functional soft-bodied jellyfish-like swimming. Nature Communications, 10, 1, 1-12. https://doi.org/10.1038/s41467-019-10549-7

[4] John H Costello, Sean P Colin, John O Dabiri, Brad J Gemmell, Kelsey N Lucas, and Kelly R Sutherland. 2020. The hydrodynamics of jellyfish swimming. Annual Review of Marine Science, 13. https://doi.org/10.1146/annurev-marine-031120-091442

[5] Jennifer Frame, Nick Lopez, Oscar Curet, and Erik D Engeberg. 2018. Thrust force characterization of free-swimming soft robotic jellyfish. Bioinspiration &

biomimetics, 13, 6, 064001. https://doi.org/10.1088/1748-3190/aadcb3
[6] Tingyu Cheng, Guori Li, Yiming Liang, Mingqi Zhang, Bangyuan Liu, Tuck-Whye Wong, Jack Forman, Mianhong Chen, Guanyun Wang, Ye Tao, and others. 2018. Untethered soft robotic jellyfish. Smart Materials and Structures, 28, 1, 015019. https://doi.org/10.1088/1361-665X/aaed4f
[7] Yara Almubarak, Matthew Punnoose, Nicole Xiu Maly, Armita Hamidi, and Yonas Tadesse. 2020. KryptoJelly: a jellyfish robot with confined, adjustable pre-stress, and easily replaceable shape memory alloy NiTi actuators. Smart Materials and Structures, 29, 7, 075011. https://doi.org/10.1088/1361-665X/ab859d
[8] Aniket Joshi, Adwait Kulkarni, and Yonas Tadesse. 2019. FludoJelly: experimental study on jellyfish-like soft robot enabled by soft pneumatic composite (SPC). Robotics, 8, 3, 56. https://doi.org/10.3390/robotics8030056
[9] Ziyu Ren, Tianlu Wang, Wenqi Hu, and Metin Sitti. 2019. A Magnetically-Actuated Untethered Jellyfish-Inspired Soft Milliswimmer. In Proceedings of Robotics: Science and Systems
[10] SN Khaderi, CB Craus, J Hussong, N Schorr, J Belardi, J Westerweel, O Prucker, J Ruhe, JM den Toonder, and PR Onck. 2011. Magnetically-actuated artificial cilia for microfluidic propulsion. Lab on a Chip, 11, 12, 2002-2010 https://doi.org/10.1039/C0LC00411A
[11] R. van Loon, P. D. Anderson, and F. N. van de Vosse. 2006. A fluid–structure interaction method with solid-rigid contact for heart valve dynamics. Journal of computational physics, 217, 806 https://doi.org/10.1016/j.jcp.2006.01.032
[12] Langquan Shui, Liangliang Zhu, Zhe Yang, Yilun Liu and Xi Chen. 2017. Energy efficiency of mobile soft robots. Soft Matter, 13, 44, 8223—8233 https://doi.org/10.1039/C7SM01617D
[13] SM Islam Khalil, Ahmet Fatih Tabak, Mohamed Abou Seif, Anke Klingner and Metin Sitti. 2018. Controllable switching between planar and helical flagellar swimming of a soft robotic sperm. PloS one, 13, 11, e0206456 https://doi.org/10.1371/journal.pone.0206456
[14] Andrew Hess, Xiaobo Tan and Tong Gao. 2020. CFD-based multi-objective controller optimization for soft robotic fish with muscle-like actuation. Bioinspiration & Biomimetics, IOP Publishing, 15, 3, 035004 https://doi.org/10.1088/1748-3190/ab6dbb
[15] Zhaowu Lin, Andrew Hess, Zhaosheng Yu, Shengqiang Cai and Tong Gao. 2019. A fluid–structure interaction study of soft robotic swimmer using a fictitious domain/active-strain method. Journal of Computational Physics, 376, 1138—1155 https://doi.org/10.1016/j.jcp.2018.10.015
[16] S. Namdeo, S. N. Khaderi, and P. R. Onck. 2013. Swimming dynamics of bidirectional artificial flagella. Phys. Rev. E, 88, 043013 https://doi.org/10.1103/PhysRevE.88.043013